Radiocarbon Measurements Reveal Underestimated Fossil CH_4 and CO_2 Emissions in London

Giulia Zazzeri[1]†, Heather Graven[1], Xiaomei Xu[2], Eric Saboya[1*], Liam Blyth[1], Alistair J. Manning[3], Hannah Chawner[4], Dien Wu[5], Samuel Hammer[6]

[1]Imperial College, Physics Department, Huxley Building, 180 Queen's Gate, South Kensington, London SW7 2AZ, United Kingdom

†Now at: ETH Zurich, Physics Department, Otto-Stern-Weg 5, 8093 Zürich, Schweiz

* Now at: School of Geographical Sciences, Bristol

[2] University of California Irvine, 2222 Croul Hall, Earth System Science

[3] Met Office, Exeter, Devon

[4] School of Chemistry, Bristol

[5] Division of Geological and Planetary Sciences, California Institute of Technology, Pasadena, USA

[6] ICOS-CRL, Institute of Environmental Physics, Heidelberg University, Im Neuenheimer Feld 229, 69120 Heidelberg, Germany

Corresponding author: Giulia Zazzeri (email: gzazzeri@phys.ethz.ch)

†Additional author notes should be indicated with symbols (current addresses, for example).

Key Points:

- Atmospheric radiocarbon measurements in central London reveal higher fossil CH_4 and CO_2 present, compared to simulations
- Radiocarbon measurements show biospheric uptake of CO_2 in July that is stronger than simulations
- Nuclear power plants interfere with radiocarbon measurements in London when air is coming from Europe

Abstract

Radiocarbon (^{14}C) is a powerful tracer of fossil emissions because fossil fuels are entirely depleted in ^{14}C, but observations of $^{14}CO_2$ and especially $^{14}CH_4$ in urban regions are sparse. We present the first observations of ^{14}C in both methane (CH_4) and carbon dioxide (CO_2) in an urban area (London) using a recently developed sampling system. We find that the fossil fraction of CH_4 and the atmospheric concentration of fossil CO_2 are consistently higher than simulated values using the atmospheric dispersion model NAME coupled with emission inventories. Observed net biospheric uptake in June-July is not well correlated with simulations using the SMURF model with NAME. The results show the partitioning of fossil and biospheric CO_2 and CH_4 in cities can be evaluated and improved with ^{14}C observations when the nuclear power plants influence is negligible.

1 Introduction

Urban environments hold more than half of the world's population and are responsible for more than 60% of greenhouse gas emissions (World Bank, 2022). Atmospheric measurements of the two major anthropogenic greenhouse gases, CO_2 and CH_4, in cities have expanded recently and emissions inventories are available at increasingly higher spatial and temporal resolutions (Minx et al. 2021). However, the attribution of emissions to specific source sectors is still largely debated and sectoral emission estimates determined using statistical approaches and associated emission factors are often found to be inconsistent with measurements (Saunois et al. 2020) . This is the case of CH_4 emissions in London, where several studies demonstrated that fossil CH_4 emissions are significantly underestimated by emission inventories (Zazzeri et al, 2017; Saboya et al. 2022). CO_2 budgets at urban scale are also difficult to resolve, as processes such as photosynthetic uptake, plant and soil respiration contribute to the net CO_2 exchange and need to be accurately quantified (Miller et al. 2020).

At Imperial College London we have measured radiocarbon (^{14}C) in both atmospheric CO_2 and CH_4. ^{14}C measurements enable partitioning of the fossil and non-fossil influences on CO_2 and CH_4. Fossil carbon is completely devoid of ^{14}C, which has all decayed during millions of years of fossil fuel formation, given a ^{14}C half-life of 5700 years. When fossil carbon is re-introduced into the atmosphere, it decreases the atmospheric $^{14}C/C$ ratio, expressed as $\Delta^{14}C$ (Stuiver and Polach, 1977), whereas biospheric influences have a much smaller impact on $\Delta^{14}C$. By measuring $\Delta^{14}C$, we can estimate carbon added from fossil fuels relative to a background site. However these measurements are challenging, especially for atmospheric CH_4, due to its relatively low concentration (~1.9 ppm) and the large amount of air needed to collect enough carbon for the ^{14}C analysis via Accelerator Mass Spectrometry (AMS). Another challenge lies in accounting for $^{14}CH_4$ and $^{14}CO_2$ emissions from nuclear power plants (NPPs). In regions where many NPPs are sited, their ^{14}C emissions can increase the atmospheric $\Delta^{14}C$ value enough to counteract the fossil carbon dilution (Eisma et al. 1995; Graven and Gruber 2011).

While $\Delta^{14}C$ has been widely used to detect regional fossil CO_2 emissions (Levin 2011, Graven et al. 2018, Wenger et al. 2019, Basu et al. 2020), only one study so far has presented a quantification of the fossil fraction of CH_4 emissions at a regional scale using ^{14}C in atmospheric CH_4 (Zazzeri et al. 2021), finding that the fossil fraction was very high in London. In that study, $\Delta^{14}CH_4$ measurements were carried out using a new methodology, which addresses the main

sampling challenge of $\Delta^{14}CH_4$ measurements by separating carbon during sampling, allowing carbon from hundreds of litres of air to be collected onto a small molecular sieve trap. The trapping method also facilitates collection of CO_2 samples for $\Delta^{14}CO_2$, enabling high precision $\Delta^{14}CO_2$ measurements (Zazzeri et al. 2021).

Here, we build on the previous study by using the same novel technique to collect atmospheric CH_4 and CO_2 samples for ^{14}C analysis between March and July 2020 in London, providing the first combined analysis of fossil CH_4 and CO_2 emissions at a regional scale using ^{14}C. We then compare the observations to model simulations with an emission inventory and biosphere model.

2 Materials and Methods

2.1 Sampling and ^{14}C analysis

CH_4 and CO_2 samples were collected using the sampling system described in Zazzeri et al. (2021). The air was sampled from an air intake on the roof of the Physics department at Imperial College London, at ~25 m height. Samples were taken in the afternoon and early evening, when air was well mixed, to avoid sampling of very local emissions. Collection of one CH_4 sample of 150 µgC took approximately 7 hours, usually from 13:00 to 20:00 (local time). CO_2 samples of ~0.5 mg C were collected at 12:00 over 30 minutes. A Picarro G2201-i analyser was used to measure the CO_2 and CH_4 mole fractions continuously from the air intake. A detailed description of the setup can be found in Saboya et al. (2022).

Sample traps were sent to the Accelerator Mass Spectrometry facilities in UC Irvine, where CO_2 was extracted and graphitised for ^{14}C analysis (Xu et al. 2007). $\Delta^{14}CH_4$ measurements are reported with uncertainties of 5 to 17 ‰, including background correction (5.5 ± 0.1 µg modern carbon, Zazzeri et al. 2021). $\Delta^{14}CO_2$ measurements are reported with uncertainties of 2 ‰, including background correction (1.5 µg of modern carbon, Zazzeri et al. 2021).

2.2 Quantification of CH_4 fossil fraction

The fossil fraction of CH_4 (i.e the ratio between fossil and total added CH_4) is calculated following the mass balance approach in Graven et al. (2019). According to this method, fossil emissions will decrease the background atmospheric $\Delta^{14}CH_4$ (~340 ‰) by a larger degree than biogenic emissions, due to the different ^{14}C signatures of fossil (-1000 ‰) and biogenic CH_4 sources (28 ±15‰, based on a turnover time of 6 ± 3 years (Lassey et al. 2007) and the $\Delta^{14}CO_2$ record (Graven et al. 2017)). Since $\Delta^{14}CH_4$ measurements of background air for 2020 were not available, we calculated the fossil fraction of differences in the CH_4 concentration between pairs of samples collected within 7-11 days with similar air provenance, either from the Atlantic or north of the UK. Thus we assumed that the background air composition was the same for each pair and the influence from NPPs was neglible as there are no NPPs in these directions. We tested the assumption that the influence from NPPs was neglible for these samples with model simulations (Section 2.5).

Three samples were collected when air was coming from Europe, where many pressurised water reactors (PWRs) that emit $^{14}CH_4$ (Zazzeri et al. 2018) are sited. These samples showed $\Delta^{14}CH_4$ higher than the most recent background observations (341‰, Sparrow et al. 2018). We did not quantify the fossil fraction for these days, but we simulated the influence of nuclear emissions

using a regional atmospheric dispersion model coupled with ^{14}C emission estimates from NPPs (see section 2.5).

2.3 Quantification of fossil and biospheric CO_2

Fossil and biospheric CO_2 are quantified using mass balances for atmospheric CO_2 concentrations and $\Delta^{14}CO_2$, following Graven et al. 2018 (Section S1). We use air samples from Mace Head, Ireland, collected by the University of Heidelberg cooperative global $^{14}CO_2$ background air network and analysed in cooperation with the Central Radiocarbon Laboratory (CRL) of the Integrated Carbon Observing System (ICOS) to define the $^{14}CO_2$ background air composition. We apply corrections for heterotrophic respiration of older carbon with higher $\Delta^{14}C$ and for NPP emissions, following Graven et al. (2018) (Section S1). Sources of NPP $^{14}CO_2$ emissions include relatively strong emissions from gas-cooled nuclear reactors in the UK and the reprocessing sites at Sellafield, UK and La Hague, France (Graven and Gruber 2011), as well as other reactor types present in the UK and Europe. We neglect biomass burning fluxes that are too small to affect our measurements (Crippa et al. 2020). Details on the quantification of NPP and heterotrophic respiration influences are given in Sections 2.4 and 2.5. Biospheric CO_2 is calculated as the difference between background CO_2 and fossil CO_2, where background CO_2 concentration is specified for individual days using a model-data technique that combines observations at Mace Head from ICOS with NAME model simulations to identify background conditions at Mace Head, with interpolation and smoothing.

2.4 CO_2 and CH_4 simulations

Model simulations were conducted using the UK Met Office's Numerical Atmospheric-dispersion Modelling Environment (NAME v7.2; Jones et al., 2007). The NAME model produces source-receptor relationships, often referred to as "footprints", for atmospheric surface measurements - i.e. the response of the observations at a measuring station to a source emission. We determined the mole fraction enhancement above background at a particular time by multiplying the footprints with CH_4 and CO_2 fluxes provided by the spatially gridded fluxes and integrating over the domain. Footprints were computed for air-histories of 30 days. Footprints used for CH_4 simulations were time-integrated over the entire 30 days, a domain of -25° to 25° longitude and 30° to 70° latitude and resolution of 0.1° x 0.1°. These footprints, combined with EDGAR emission inventories, produced the best match between simulated CH_4 concentrations and our CH_4 observations in London (Saboya et al. 2022). Footprints used for CO_2 simulations had hourly resolution in the first 24 hours and 29-day integration thereafter, a domain of -97.9° to 39.4 ° longitude and 10.73° to 79.05°latitude, and a resolution of 0.23° x0.35° (White et al. 2019). Footprints can be found in section S3 of the supplementary material.

For CH_4 fluxes, we used monthly CH_4 fluxes from EDGARv6. We calculate fossil CH_4 (sectors: aviation, ship, coal, gas, oil, energy, chemical processes, fossil fuel building, fossil fuel fire) and total CH_4 enhancements separately and compute a simulated fossil fraction of CH_4 present. As with the observations, we compared between pairs of simulated CH_4 corresponding to the observation pairs.

For fossil fuel CO_2 fluxes, we used monthly fossil fuel emissions from EDGARv4.3 and resolved the monthly emissions into hourly emissions, accounting for the seasonal, weekly and daily variability in CO_2 emissions based on the UKGHG model (White et al. 2019).

For biospheric CO_2 fluxes, we used hourly mean net ecosystem exchange (NEE) fluxes from the Solar-Induced Fluorescence for Modeling Urban biogenic Fluxes ("SMUrF") Model (Wu et al. 2021). For the heterotrophic respiration correction term, heterotrophic respiration fluxes were approximated from the NEE and the mean gross primary production (GPP) fluxes ([GPP+NEE]/2) from SMUrF. $\Delta^{14}C$ of heterotrophic respiration was assumed to be 50 ± 35 ‰ (Section S1, Graven et al. 2018).

2.5 ^{14}C Enhancements from NPPs

The ^{14}C enhancement due to the emissions from NPPs was also simulated using the NAME footprints. The $^{14}CO_2$ and $^{14}CH_4$ emissions were specified in two ways: 1. using emission factors based on electrical power production, and 2. with ^{14}C measurements sourced from the European Commission RAdioactive Discharges Database (RADD 2020).

When using emission factors, we followed the S1 emission factor database in Zazzeri et al. 2018. We attributed two different emission factors to PWRs, based on the reactor model: 0.407± 0.198 TBq/GWa for VVER (Russian design) and 0.193 ± 0.061 TBq/GWa for non-VVER reactors. Emission factors were multiplied by 2020 energy outputs retrieved from the International Atomic Energy Agency's Power Reactor Information System (IAEA PRIS 2020). Finally, the ^{14}C estimates were scaled down by a factor of 53 % to represent the $^{14}CH_4$ proportion of total ^{14}C emissions from PWRs (Kunz 1985, Zazzeri et al. 2018), and by a factor of 28% for $^{14}CO_2$ emissions from PWRs. We used the Graven and Gruber (2011) emission factors to estimate $^{14}CO_2$ from Gas-cooled reactors (GCRs), advanced Gas-cooled reactors (AGRs) in the UK and Boiling water reactors (BWRs) in Europe, assuming all ^{14}C emissions to be $^{14}CO_2$. The $^{14}CO_2$ release from two reprocessing plants, one in the La Hague in France and one in Sellafield in the UK, were retrieved from the RADD database.

3 Results

3.1 $\Delta^{14}CH_4$ measurements and Fossil Fraction of CH_4

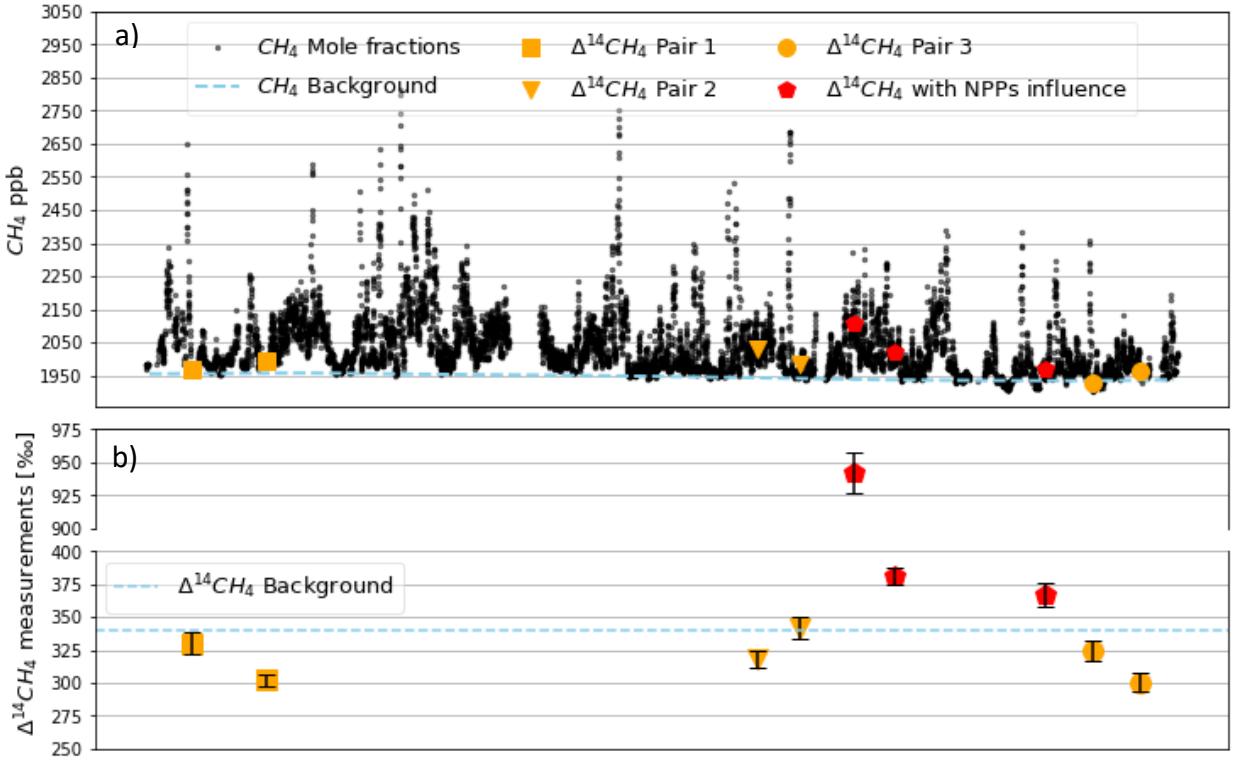

Figure 1: a) Continuous record of 20 min averaged CH_4 mole fraction measurements (black), CH_4 mole fractions of collected samples used for quantification of the fossil fraction (orange), CH_4 mole fraction of samples influenced by $^{14}CH_4$ emissions from NPPs (red), CH_4 mole fraction of background values measured at Mace Head (blue line) and fitted according to Manning et al. 2021. b) $\Delta^{14}CH_4$ values of collected samples using the same color coding, expected background $\Delta^{14}CH_4$ of 340 ±4‰ (blue line), error bars in black.

Figure 1 shows the continuous record of CH_4 mole fractions measured at Imperial College London over the study period and $\Delta^{14}CH_4$ values of the samples collected. Sample pairs with measured $\Delta^{14}CH_4$ below the expected background level and air provenance from the north or west UK were used for quantification of the CH_4 fossil fraction of the emissions (Table 1). Samples with measured $\Delta^{14}CH_4$ above the expected background level were not included.

Table 1: Measured FF of sample pairs collected in London in 2020. The uncertainty on the FF has been calculated propagating the error on the $\Delta^{14}C$ values and mole fraction measurements (section S5).

Dates	Air Provenance	Measured ΔCH_4 (ppb)	Simulated ΔCH_4 (ppb)	Measured $\Delta\Delta^{14}C$ (‰)	Calculated $ffCH_4$ (ppb)	Measured relative FF (%)	Simulated relative FF (%)
7 & 18 March	Atlantic	25 ± 3	2	28 ± 9	47 ±18	186 ± 77	44
29 May & 4 June	North UK	47 ± 3	59	24 ± 10	32 ±20	69 ± 43	4

17 & 24 July	Atlantic	36± 1	1.2	24 ± 10	36 ±20	99 ± 55	11

A fossil fraction (FF) of 99 % and higher was calculated from two pairs of samples collected when air was coming from the Atlantic, and 69 % for one pair collected when air was coming from the north (Table 1). Here the fossil fraction is for the CH_4 added between the day with higher CH_4 and the day with lower CH_4, assuming the two days had similar background air composition (same air provenance) and a negligible NPP influence (see Table S1). Estimated background CH_4 concentrations at the Mace Head station were also comparable for each pair. The simulated FF for the CH_4 difference between the pairs of samples is smaller than the measured FF, meaning that the EDGAR v6 inventory coupled with the NAME model tend to underestimate fossil CH_4 emissions, similar to the result in Saboya et al. 2022 using $\delta^{13}CH_4$ data. The simulated CH_4 mole fraction difference for each pair is also not consistent with the measured one, being considerably smaller when air came from the Atlantic but slightly higher when air came from the north. The main source of uncertainty in the fossil fraction is the $\Delta^{14}CH_4$ measurement uncertainty, which is in the range of 5 to 9 ‰.

$\Delta^{14}CH_4$ measurements on 12 June, 18 June and 10 July were higher than the expected background level and NAME simulations indicated they were affected by nuclear power plant emissions (Table S1). The measurement on 12 June was particularly high (942 ± 17 ‰). According to the NAME footprints, on 12 June air was coming from Germany, passing through Belgium and then Suffolk, England, where the PWR Sizewell B is located. Sizewell B was offline for a planned outage for a period including 12 June and high emissions are expected during the first weeks of a temporary shut down of the reactor (Lehmuskoski et al. 2021).

3.2 $\Delta^{14}CO_2$ measurements and fossil and biospheric CO_2

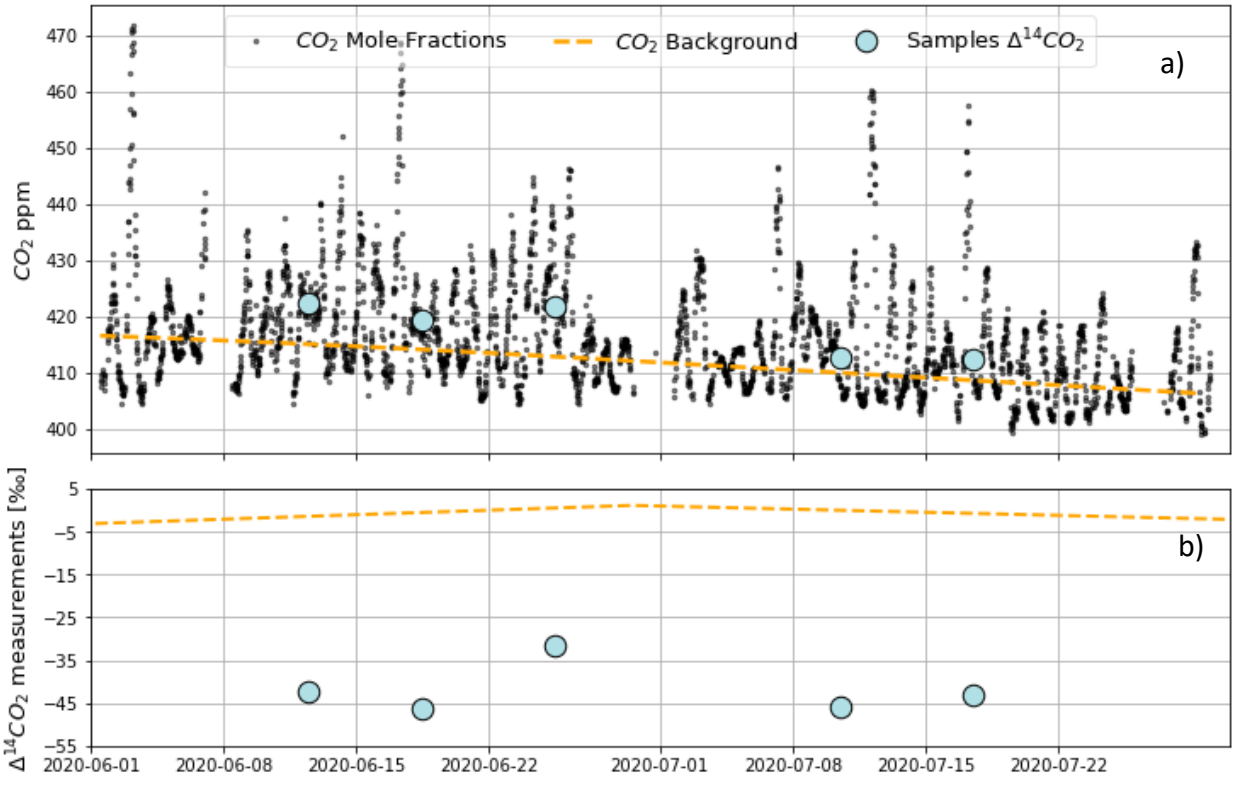

Figure 2: a) Continuous record of 20 min averaged CO_2 mole fraction measurements (black), CO_2 mole fractions of collected samples (light blue), CO_2 mole fraction of background values measured at Mace Head (orange line); b) $\Delta^{14}CO_2$ values of collected samples (light blue). $\Delta^{14}CO_2$ of air collected at Mace Head over June and first week of July in orange.

$\Delta^{14}CO_2$ observations in summer 2020 span a range between -46.2 and -31.5 ‰ (Figure 2), lower than the Mace Head data around 0 ‰, similar to reported $\Delta^{14}CO_2$ depletions in large conurbations such as Los Angeles (Miller et al. 2020). The added $ffCO_2$ of samples is between 12 and 20 ppm, whereas the simulated added $ffCO_2$ is between 1 and 10 ppm (Table 3).

It is possible that very local emissions, such as CO_2 emissions from a gas-fired power plant located 200 metres east of our inlet, could interfere with our measurements. However, according to Sparks and Toumi (2010), the emission plume from the power station would cross our air inlet only for easterly winds, and with a bigger effect for moderate wind speeds (3 – 5 m/s). At lower wind speed the plume is going upwards and is not intersecting with our air inlet (see supplementary material for the CO_2 mole fraction record and wind data).

Table 3 includes the applied nuclear (β_{NPP}) and the heterotrophic respiration (β_{HR}) correction terms on the final fossil CO_2 mole fraction ($ffCO_2$) expressed as ppm of $ffCO_2$. The nuclear correction is within the uncertainty of $ffCO_2$. The highest value is on 18 June when air is coming from northern France, where the La Hague reprocessing plant is sited, which, according to the RADD database, releases about 80% of the total ^{14}C release from NPPs in Europe and the UK. The correction for heterotrophic respiration is within 1 ppm, higher in June.

All samples show a negative biospheric CO_2 contribution (Cveg in Table 3), indicating that the biosphere acts as a net sink, taking up from 3-17 ppm. The simulated biospheric contribution is also negative, but there are significant differences in the magnitude of Cveg between the simulations and observations. The CO_2 uptake is stronger in June in the simulations, partly due to more influence from Europe (Figure S3), but not in the observations. In the simulations, the London urban region accounts for 15-44% of the biospheric uptake.

Table 2: $\Delta^{14}CO_2$ measurements of samples collected in London in 2020, calculated and simulated $ffCO_2$ and Cveg, and the NPP and heterotrophic correction terms (β_{NPP} and β_{HR}). The uncertainties on $ffCO_2$ and Cveg have been calculated by propagating the error on the $\Delta^{14}C$ values and mole fraction measurements and the correction terms (Graven et al. 2018).

Date	CO_2 (ppm)	$\Delta^{14}CO_2$ (‰)	Meas $ffCO_2$ (ppm)	Sim $ffCO_2$ (ppm)	Meas Cveg (ppm)	Sim Cveg (ppm)	β_{NPP} (ppm)	β_{HR} (ppm)
12/06/2020	422.2 ±2.2	-42.3 ±1.4	17.0 ±1.0	8.6	-9.8 ±1.0	-14.5	0.16 ±0.05	0.57 ±0.4
18/06/2020	419.4 ±2.0	-46.3 ±1.8	19.4 ±1.1	9.6	-14.0 ±1.1	-24.0	0.83 ±0.31	0.57 ±0.4
25/06/2020	421.8 ±0.5	-31.5 ±2.0	12.3 ±1.1	6.6	-3.3 ±1.2	-8.6	0.03 ±0.04	0.44 ±0.4
10/07/2	412.7	-46.2	19.6	1.2	-16.8	-7.8	$2 \cdot 10^{-5}$	0.06

020	±0.1	±1.6	±1.0		±1.0			
17/07/2020	412.2 ±0.3	-43.2 ±1.6	18.4 ±0.9	1.4	-14.8 ±1.0	-6.5	$3 \cdot 10^{-6}$	0.13

4 Discussion and Conclusions

In this work we provide the first source characterisation of CH_4 and CO_2 using both $\Delta^{14}CH_4$ and $\Delta^{14}CO_2$ measurements, utilizing a new sampling system (Zazzeri et al. 2021). This study demonstrates the power of ^{14}C observations to attribute the fossil fuel influence on both CO_2 and CH_4, and that our atmospheric station in central London is well-suited for such measurements as long as sampling days are selected to minimize the influence of nearby nuclear reactors and the La Hague fuel reprocessing site.

The fossil fraction of added CH_4 was very high in sample pairs with air provenance from the Atlantic or north of the UK that had no NPP influence. Simulated fossil fractions of added CH_4 between the samples in each pair were much lower, demonstrating that the EDGARv6 emissions inventory is likely to underestimate fossil CH_4 in the London region, similar to prior studies finding underestimated natural gas emissions in London (Saboya et al. 2022, Zazzeri et al. 2017, Helfter et al. 2016). However, the uncertainty on the calculated CH_4 fossil fraction is high. Improvements in $\Delta^{14}CH_4$ measurements and higher CH_4 enhancements would improve the fossil fraction uncertainty.

Our $\Delta^{14}CO_2$ observations show that during summer in London the biosphere acts as a net sink of CO_2 that strongly counteracts the influence from fossil fuel emissions. This highlights the importance of tracer measurements such as $\Delta^{14}CO_2$ for isolating fossil fuel CO_2 in urban areas where urban or regional vegetation can have a significant impact on CO_2 concentrations. As expected, the $ffCO_2$ concentrations we observed in London (12 to 20 ppm) are much higher than those observed at a rural site in the UK, which were comparable to the measurement uncertainty (~2 ppm, Wenger et al. 2019). Observations of $ffCO_2$ using $\Delta^{14}CO_2$ in other large urban areas, for example, in Los Angeles, show similar average values on the order of 10 ppm (Miller et al. 2020; Graven et al. 2018). The comparison of observed $ffCO_2$ and $bioCO_2$ with simulations in London showed strong discrepancies, where a primary cause is likely to be the low resolution of the NAME atmospheric model, but also potentially low resolution or errors in the fossil fuel and biospheric fluxes in the EDGAR inventory and SMURF model. This study shows how interpretation of in situ or satellite CO_2 measurements in urban areas requires tracer measurements such as $\Delta^{14}CO_2$ for quantifying fossil fuel and biospheric CO_2, as well as high resolution atmospheric modelling and high resolution prior flux maps.

Acknowledgments

This project was funded by the European Research Council (ERC) under the European Union's Horizon 2020 research and innovation programme (grant agreement 67910).

299 NAEI inventories were retrieved from the NAEI website:
300

301 **Open Research**

302 The data used for this study include the observations at Imperial College London, radiocarbon
303 measurements and simulated values using the Met Office model NAME. They are in a .csv
304 format and available at the following repository:

305 https://doi.org/10.5281/zenodo.7777987

306 Data are accessible to the general public without any restrictions.

307 Figures were made with Matplotlib 3.6.0. (https://matplotlib.org/). Maps in the supplementary
308 material were made using Matplotlib with Cartopy (https://pypi.org/project/Cartopy/).

309
310 **References**

311 Basu, S., Lehman, S.J., Miller, J.B., Andrews, A.E., Sweeney, C., Gurney, K.R., Xu, X.,
312 Southon, J. and Tans, P.P. (2020). Estimating US fossil fuel CO_2 emissions from measurements
313 of ^{14}C in atmospheric CO_2. Proceedings of the National Academy of Sciences, 117(24), 13300-
314 13307.

315 Crippa, M., Solazzo, E., Huang, G., Guizzardi, D., Koffi, E., Muntean, M., Schieberle, C.,
316 Friedrich, R. and Janssens-Maenhout, G. (2020). High resolution temporal profiles in the
317 Emissions Database for Global Atmospheric Research. Scientific data, 7(1), 1-17.

318 Eisma, R., Vermeulen, A.T. and Van Der Borg, K. (1995). $^{14}CH_4$ emissions from nuclear power
319 plants in northwestern Europe. Radiocarbon, 37(2), pp.475-483.

Graven, H. D., & Gruber, N. (2011). Continental-scale enrichment of atmospheric $^{14}CO_2$ from the nuclear power industry: potential impact on the estimation of fossil fuel-derived CO_2. Atmospheric Chemistry and Physics, 11(23), 12339-12349.

Graven, H., Allison, C.E., Etheridge, D.M., Hammer, S., Keeling, R.F., Levin, I., Meijer, H.A., Rubino, M., Tans, P.P., Trudinger, C.M. and Vaughn, B.H. (2017). Compiled records of carbon isotopes in atmospheric CO_2 for historical simulations in CMIP6. Geoscientific Model Development, 10(12), pp.4405-4417.

Graven, H., Fischer, M.L., Lueker, T., Jeong, S., Guilderson, T.P., Keeling, R.F., Bambha, R., Brophy, K., Callahan, W., Cui, X. and Frankenberg, C. (2018). Assessing fossil fuel CO_2 emissions in California using atmospheric observations and models. Environmental Research Letters, 13(6), p.065007.

Graven, H., Hocking, T., & Zazzeri, G. (2019). Detection of fossil and biogenic methane at regional scales using atmospheric radiocarbon. Earth's future, 7(3), 283-299.

Helfter, C., Tremper, A.H., Halios, C.H., Kotthaus, S., Bjorkegren, A., Grimmond, C.S.B., Barlow, J.F. and Nemitz, E. (2016). Spatial and temporal variability of urban fluxes of methane, carbon monoxide and carbon dioxide above London, UK. Atmospheric Chemistry and Physics, 16(16), pp.10543-10557.

Jones, A., Thomson, D., Hort, M., & Devenish, B. (2007). The UK Met Office's next-generation atmospheric dispersion model, NAME III. In Air pollution modeling and its application XVII (pp. 580-589). Springer, Boston, MA.

Kunz, C. (1985). Carbon-14 discharge at three light-water reactors. Health Physics, 49(1), 25-35.

Lassey, K. R., Lowe, D. C., & Smith, A. M. (2007). The atmospheric cycling of radiomethane and the" fossil fraction" of the methane source. Atmospheric Chemistry and Physics, 7(8), 2141-2149.

Lehmuskoski, J., Vasama, H., Hämäläinen, J., Hokkinen, J., Kärkelä, T., Heiskanen, K., Reinikainen, M., Rautio, S., Hirvelä, M. and Genoud, G. (2021). On-Line Monitoring of

346 Radiocarbon Emissions in a Nuclear Facility with Cavity Ring-Down Spectroscopy. Analytical
347 Chemistry, 93(48), pp.16096-16104.

348 Levin, I., Münnich, K. O., & Weiss, W. (1980). The effect of anthropogenic CO2 and 14C
349 sources on the distribution of 14C in the atmosphere. Radiocarbon, 22(2), 379-391.

350 Levin 2011 Phil. Trans. R. Soc. A (2011) 369, 1906–1924

351 Manning, A.J., Redington, A.L., Say, D., O'Doherty, S., Young, D., Simmonds, P.G., Vollmer,
352 M.K., Mühle, J., Arduini, J., Spain, G. and Wisher, A. (2021). Evidence of a recent decline in
353 UK emissions of hydrofluorocarbons determined by the InTEM inverse model and atmospheric
354 measurements. Atmospheric Chemistry and Physics, 21(16), pp.12739-12755.

355 Miller, J.B., Lehman, S.J., Verhulst, K.R., Miller, C.E., Duren, R.M., Yadav, V., Newman, S.
356 and Sloop, C.D. (2020). Large and seasonally varying biospheric CO2 fluxes in the Los Angeles
357 megacity revealed by atmospheric radiocarbon. Proceedings of the National Academy of
358 Sciences, 117(43), 26681-26687.

359 Minx, J.C., Lamb, W.F., Andrew, R.M., Canadell, J.G., Crippa, M., Döbbeling, N., Forster,
360 P.M., Guizzardi, D., Olivier, J., Peters, G.P. and Pongratz, J. (2021). A comprehensive and
361 synthetic dataset for global, regional, and national greenhouse gas emissions by sector 1970–
362 2018 with an extension to 2019. Earth System Science Data, 13(11), 5213-5252.

363 Saboya, E., Zazzeri, G., Graven, H., Manning, A. J., & Englund Michel, S. (2022). Continuous
364 CH 4 and δ 13 CH 4 measurements in London demonstrate under-reported natural gas leakage.
365 Atmospheric Chemistry and Physics, 22(5), 3595-3613.

366 Saunois, M., Stavert, A.R., Poulter, B., Bousquet, P., Canadell, J.G., Jackson, R.B., Raymond,
367 P.A., Dlugokencky, E.J., Houweling, S., Patra, P.K. and Ciais, P. (2020). The global methane
368 budget 2000–2017. Earth system science data, 12(3), pp.1561-1623.

369 Sparks, N. and Toumi, R. (2010). Remote sampling of a CO_2 point source in an urban setting.
370 Atmospheric Environment, 44(39), pp.5287-5294.

Sparrow, K.J., Kessler, J.D., Southon, J.R., Garcia-Tigreros, F., Schreiner, K.M., Ruppel, C.D., Miller, J.B., Lehman, S.J. and Xu, X. (2018). Limited contribution of ancient methane to surface waters of the US Beaufort Sea shelf. Science advances, 4(1), p.eaao4842.

Stuiver, M., & Polach, H. A. (1977). Discussion reporting of 14C data. Radiocarbon, 19(3), 355-363.

Wenger, A., Pugsley, K., O'Doherty, S., Rigby, M., Manning, A. J., Lunt, M. F., & White, E. D. (2019). Atmospheric radiocarbon measurements to quantify CO_2 emissions in the UK from 2014 to 2015. Atmospheric Chemistry and Physics, 19(22), 14057-14070.

White, E.D., Rigby, M., Lunt, M.F., Smallman, T.L., Comyn-Platt, E., Manning, A.J., Ganesan, A.L., O'Doherty, S., Stavert, A.R., Stanley, K. and Williams, M., (2019). Quantifying the UK's carbon dioxide flux: an atmospheric inverse modelling approach using a regional measurement network. Atmospheric Chemistry and Physics, 19(7), pp.4345-4365.

World Bank (2022), “Urban development”, available at: www.worldbank.org/en/topic/urbandevelopment/overview (accessed 02 March 2023).

Wu, D., Lin, J. C., Oda, T., & Kort, E. A. (2020). Space-based quantification of per capita CO_2 emissions from cities. Environmental Research Letters, 15(3), 035004.

Wu, D., Lin, J. C., Duarte, H. F., Yadav, V., Parazoo, N. C., Oda, T., & Kort, E. A. (2021). A model for urban biogenic CO_2 fluxes: Solar-Induced Fluorescence for Modeling Urban biogenic Fluxes (SMUrF v1). Geoscientific Model Development, 14(6), 3633-3661.

Xu, X., Trumbore, S. E., Zheng, S., Southon, J. R., McDuffee, K. E., Luttgen, M., & Liu, J. C. (2007). Modifying a sealed tube zinc reduction method for preparation of AMS graphite targets: reducing background and attaining high precision. Nuclear Instruments and Methods in Physics Research Section B: Beam Interactions with Materials and Atoms, 259(1), 320-329.

Zazzeri, G., Lowry, D., Fisher, R. E., France, J. L., Lanoisellé, M., Grimmond, C. S. B., & Nisbet, E. G. (2017). Evaluating methane inventories by isotopic analysis in the London region. Scientific reports, 7(1), 1-13.

Zazzeri, G., Yeomans, E. A., & Graven, H. D. (2018). Global and regional emissions of radiocarbon from nuclear power plants from 1972 to 2016. Radiocarbon, 60(4), 1067-1081.

Zazzeri, G., Xu, X., & Graven, H. (2021). Efficient Sampling of Atmospheric Methane for Radiocarbon Analysis and Quantification of Fossil Methane. Environmental Science & Technology, 55(13), 8535-8541.